Disorder and localization in ribbed structures with fluid loading

By Mark Spivack and Paul E. Barbone

Department of Applied Mathematics and Theoretical Physics, University of Cambridge, Silver Street, Cambridge CB3 9EW, U.K.

The paper considers the steady-state harmonic response of an elastic fluid-loaded membrane supported by irregularly spaced ribs. Under the assumption of subsonic wave coupling, the solution is given exactly for any configuration as a product of 2×2 transfer matrices. It is well known that the response of a periodically ribbed membrane exhibits a pass/stop band structure. Although this structure is destroyed in the irregular case, we find that two distinct régimes remain: smooth and fluctuating exponential decay. The transfer matrix solution is used to explain these regions. The average transfer matrix is obtained exactly; where the decay is smooth its eigenvalues approximately determine the localization length.

1. Introduction

This paper considers the problem of wave propagation along a fluid loaded elastic membrane which is supported by an irregular array of ribs. One of the ribs is driven by a time-harmonic force and the rest have infinite mechanical impedance. Coupling between bays is provided purely by fluid loading. This and related problems have been widely studied (see, for example, Crighton 1983, 1984, 1988; Crighton & Maidanik 1981; Eatwell & Willis 1982; Mace 1980; Photiadis 1992; Sobnack 1991; Spivack 1991). The Green function (Crighton 1983, 1984) for the fluid-loaded membrane consists of an acoustic component G_a and a subsonic surface wave component G_s; attention here will be restricted to régimes in which G_a can be neglected at distances comparable with the rib spacing. The only method of solution previously presented in the literature is by numerical inversion of the governing matrix equation. In such systems this procedure is extremely sensitive to rounding errors, and rapidly becomes prohibitive for large arrays.

When the ribs are periodically spaced (see Crighton 1984; Sobnack 1991) the frequency response of the system falls into stop bands, in which energy is exponentially localized about the driving force, and pass bands, in which energy propagates without attenuation. For finite periodic arrays the behaviour has considerable complexity, and the detailed solution (Spivack 1991) exhibits high sensitivity to driving frequency. Irregularity introduces exponential localization of surface waves at all frequencies. Sobnack (1991) and Sobnack & Crighton (1994) derived analytical expressions for the decay length for small and large disorder, and noticed that the average response in the stop band is insensitive to structural irregularity.

The purpose of this paper is to present an exact solution for structures with

Proc. R. Soc. Lond. A (1994), **444**, 73–89
Printed in Great Britain

arbitrary rib spacing under the assumption of subsonic wave coupling, and to elucidate important features of the response. In particular it is shown that the response remains highly dependent upon frequency. By manipulation of the governing matrix equation, the force at any rib can be expressed in terms of the forces at two adjacent ribs. This gives rise to a sequence of 2×2 transfer matrices, which act successively on adjacent pairs of rib forces. The solution is thus evaluated from the free end of the array towards the driving force, and at that point a normalizing factor is determined which completes the solution. This is directly analogous to the situation for a regular array. From this description the effect upon the system of any changes of configuration is easily seen; moving one rib affects only the forces upstream (towards the driving force), apart from the multiplying factor which is constant along the array.

There are two distinct localization régimes, in which the decay is either *smooth* or *fluctuating*. These correspond roughly to frequencies lying in the stop and pass bands, respectively, and the transition between them occurs over a small frequency band. When the decay is smooth, the typical response is insensitive to structural disorder. This behaviour can be understood in terms of the transfer matrices: smooth decay occurs where one eigenvalue is dominant and the eigenvalues are narrowly distributed about the mean. Furthermore, the stop band response typically shows a slight *decrease* in localization with disorder. It follows that for every degree of disorder there are 'stationary frequencies' at which the decay rate is equal to that of the regular case. At such frequencies, the decay length at first increases with disorder and then decreases again.

In §2 the mathematical formulation is given and the statistical models are described. The general exact solution is given in §3. This is followed by a calculation of the mean transfer matrix, treating the rib-spacings as independent random variables. In §4 the effects of disorder are considered and illustrated, including the degree and qualitative nature of localization, and a comparison is made between the eigenvalues of the mean transfer matrix and the decay rate.

2. Mathematical formulation

(*a*) *Physical model and governing equations*

Full details of the physical model and properties of the Green function are given elsewhere (e.g. Crighton 1983, 1984; Sobnack 1991) and will not be repeated at length here. Notation follows that of Spivack (1991). We consider an elastic membrane which lies in the plane $y = 0$, bounding a quiescent compressible fluid in the half-space $y > 0$ and a vacuum in $y < 0$. The membrane is supported by N thin ribs along the lines $x_m = mh + u'_m$ where $m = 1, \ldots, N$, and the displacements u'_m may be deterministic or drawn from some statistical distribution (see §2*b*). We may assume that $u'_1 = 0$. The rib at x_1 is driven with a prescribed velocity in the y-direction by a time-harmonic line-force. The solution for a force applied at any other rib may be obtained in almost exactly the same way as here and shows no qualitative difference. All ribs other than that at x_1 have infinite mechanical impedance. Fluid loading is therefore the only mechanism by which energy can be transmitted across any non-driven rib. A harmonic time-dependence $\exp(-\mathrm{i}\omega t)$ is to be understood throughout. The force on the membrane due to the mth rib is denoted F_m. $V(x)$ is the normal velocity of the fluid-loaded membrane, and G is the corresponding Green function. It

will be assumed that $V(x_1)$, the velocity of the driven rib, is known. (The solution of the related problem in which the force F_1 is prescribed is obtained in the same way simply by renormalizing throughout by F_1.) By convention x increases from left to right, and the driven rib is at the left-hand end.

Adopting the notation in Crighton (1984), $G = G_a + G_s$, where G_a, G_s are the acoustic and subsonic wave contributions to the Green function, respectively. κ is the wavenumber of the subsonic surface wave which propagates on the fluid-loaded membrane. Crighton shows that G_a can be neglected except at small arguments. Thus for $\kappa|x| \gg 1$, G is given by

$$G(x) \sim G_s(x) = A_\infty \exp(\mathrm{i}\kappa|x|).$$

Similarly, we take $G(0) = G_s(0) + G_a(0) = A_0$. The constants A_∞, A_0 are given in Crighton (1984) and are not needed explicitly here.

We seek the solution for the forces F_m. These determine the structural response everywhere since F_m and V are related by

$$V(x) = \sum_{n=1}^{N} F_n G(x - x_n). \tag{1}$$

Since $V(x_m)$ is known for all m we can obtain a matrix equation from which the forces can be determined. The problem may be scaled so that the velocity at x_1 is unity, the factors A_∞, A_0 simplify, and the reference rib-spacing h is subsumed into the scaled driving frequency ϕ in such a way that in the absence of disorder the rib locations are given by $x_n = n$. We thus obtain

$$\boldsymbol{W} = A\boldsymbol{F}. \tag{2}$$

Here $\boldsymbol{W} = (1, 0, \ldots, 0)$ is the vector of scaled velocities, $\boldsymbol{F} = \{F_n\}$ is the vector of forces, and A is the symmetric $N \times N$ matrix given by

$$A_{jk} = \exp(\mathrm{i}\phi|x_j - x_k|), \quad \text{for} \quad j \neq k$$

with diagonal

$$A_{kk} = 1 - \mathrm{i}/\sqrt{3}.$$

The method of solution presented in this paper does not depend on the assumed form of the diagonal elements. In the examples to follow, these are chosen to correspond to the low frequency range of heavy fluid loading (Crighton 1984).

The rib-spacing is denoted by $\delta_n \equiv x_n - x_{n-1}$ so that with no disorder $\delta_n = 1$, and displacements of the ribs from the periodic configuration by $u_n = x_n - n$. We define $z = \exp(\mathrm{i}\phi)$, $\beta = A_{kk} = 1 - \mathrm{i}/\sqrt{3}$ and denote the mth row of A by $\boldsymbol{A}_m$. The matrix equation (2) represents N linear equations, denoted $[1] \ldots [N]$, which are of the form

$$\boldsymbol{A}_m \cdot \boldsymbol{F} = \delta_{1m}, \qquad [m]$$

where δ_{1m} is the Kronecker delta. Explicitly, for $N \geqslant m > 1$ this can be written as

$$z^{x_m - x_1}E_1 + \ldots + z^{x_m - x_{m-1}}E_{m-1} + \beta E_m + z^{x_{m+1} - x_m}E_{m+1} + \ldots + z^{x_N - x_m}E_N = 0. \tag{3}$$

Here we have introduced the *normalized forces* E_m, defined as $E_m = F_m/F_N$.

We recall briefly the characteristics of the response of a fluid-loaded elastic membrane supported by a finite periodic array of ribs (Spivack 1991). The frequency in this case can be assumed to lie in $[0, 2\pi)$, and this range is divided into *stop bands*,

where the rib forces decay exponentially away from the driving force, and *pass bands*, where the forces fluctuate from one rib to the next, but without overall attenuation. The stop bands are $(0, \frac{2}{3}\pi)$, and $(\pi, \frac{5}{3}\pi)$, and the remaining open intervals are the pass bands. The band edges themselves possess quite distinct responses and do not strictly conform to either band. These regions correspond to the properties of the transfer matrices: at pass band frequencies the eigenvalues lie on the complex unit circle, whereas in the stop band they are real, their product is one, and the larger one determines the rate of decay. By contrast, in irregular systems the response becomes attenuated at all frequencies. For convenience, however, we will continue to refer to these frequency ranges as stop and pass bands.

(*b*) *Statistical models*

To characterize the degree of disorder we need a statistical description of the irregular structure. We will suppose here that the rib locations depart from periodicity according to some distribution such that 'on average' the arrangement is periodic. The governing equations can be written in terms of rib positions x_n, displacements u_n from periodicity, or bay lengths (rib spacings) δ_n.

Each array is to be thought of as member of an ensemble of random processes, and averages are taken over the ensemble unless stated otherwise. The ensemble average throughout is denoted by angled brackets $\langle \ldots \rangle$. The problem is most easily discussed in terms of independent sets of random variables. (For example $\{u_n\}$ is independent if $\langle u_n u_m \rangle = \langle u_n \rangle \langle u_m \rangle$ for $m \neq n$.) The sets $\{u_n\}$ and $\{\delta_n\}$ cannot simultaneously be independent.

There are two obvious models for the disorder. In one, the random displacements u_n are drawn independently from some distribution with mean zero. Since ribs cannot overlap this restricts $|u_n|$ to be less than $\frac{1}{2}$. Sobnack (1991) adopts this model with the uniform distribution on $[-\Delta, \Delta]$. This will be referred to as *model* 1. Following Sobnack the degree of disorder will be defined by Δ. (For more general distributions it is more natural to define the disorder as the r.m.s. variation $\langle u_n^2 \rangle^{\frac{1}{2}}$, which in this case is $\Delta/\sqrt{3}$.) As indicated above choosing the u_ns independently introduces a correlation between successive rib spacings δ_n: a large bay will tend to be followed by a small bay (and conversely).

In the second model the bay lengths $\delta_n = x_{n+1} - x_n$ are allowed to vary independently, according to some positive distribution with mean 1. For our results δ_n is chosen uniformly from $[1-\Delta, 1+\Delta]$ where Δ is less than 1. Again the degree of disorder is defined to be Δ. This will be referred to as *model* 2. It is more flexible in that the ensemble contains that of model 1 as a subset, and also allows greater disorder. In this case the rib displacements $x_n - n$ describe a random walk, and although x_n again has mean n, displacements to the right may now be arbitrarily large, so that the variance of x_n about its mean value n grows unboundedly with n.

These models are sufficiently general for most purposes. For small disorder there is no qualitative difference between the resulting response. In practice the choice between them may be governed by the envisaged application: thus we would apply model 1 if all rib positions are measured from a fixed point to within an absolute (not percentage) tolerance, and model 2 if each rib is placed in relation to the previous one.

Note that the mean $\langle A \rangle$ of a linear operator A is the operator B such that $\langle Af \rangle \equiv Bf$ for any fixed vector f. It follows that the mean of a matrix is given by the mean of its elements. Finally (see, for example, Papoulis 1981), given any

function g of n independent random variables $X_1, \ldots, X_n$, with distribution functions $f_i, i = 1, \ldots, n$ respectively, the mean of g can be written

$$\langle g \rangle = \int_{-\infty}^{\infty} \ldots \int_{-\infty}^{\infty} g(X_1, \ldots, X_n) f_1 \ldots f_n \, \mathrm{d}X_1 \ldots \mathrm{d}X_n.$$

3. General solution

In this section we obtain the exact solution for the forces along a finite irregular array. We first rearrange the system of equations [1] to [N] in order to express the force at each rib in terms of its nearest neighbours. This gives rise to a succession of 2×2 transfer matrices. From these we obtain the normalized forces $E_n = F_n/F_N$, for all $n \geqslant 2$. Finally the normalized driving force E_1 and the end force F_N are obtained, both of which are expressly coupled to all other ribs. This completes the solution. Later in this section we will evaluate the average transfer matrix $P = \langle P_n \rangle$, and compare its eigenvectors and eigenvalues with the analogous quantities for a periodic array.

We restrict ourselves for simplicity to the case in which the driven rib is at one end of the array. The analysis changes little when the Mth rib, say, is driven, and the results are qualitatively identical. The extension to this more general case is exactly analogous to the corresponding extension for a periodic array (Spivack 1991): equations [1] to [$M-1$] are normalized by F_1, and equations [$M+1$] to [N] by F_N. This enables us to find the forces to the left and right of F_M, normalized by F_1 and F_N respectively. It is then straightforward to find F_1, F_M, F_N and thus complete the solution.

The method presented here is analogous to the treatment for a periodic array (Spivack 1991). The transfer matrix in that case remains constant along the array and all forces can be expressed in closed form. This is of course not possible in the irregular case because the solution depends upon arbitrarily many independent rib displacements. An intermediate case, in which a single rib in a periodic system is displaced, has been tackled using a similar formulation by Sobnack (1991), and Sobnack & Crighton (1993).

(*a*) *Exact solution for an arbitrary array*

The expressions which describe the transmission along the structure are now derived. The main quantities will be written in terms of x_n or δ_n as is convenient. The procedure is similar to the regular case, adapted here to take account of the additional algebraic structure due to disorder. The calculation is straightforward but notationally cumbersome, and unnecessary details will be omitted.

(i) *Normalized forces at the last two ribs*

The force F_{N-1} at the penultimate rib can be found in terms of that at the end-rib F_N by a simple manipulation of (2). To do so, we multiply equation [$N-1$] by the factor z^{δ_N} and subtract the result from equation [N], obtaining

$$F_{N-1} = \mu F_N, \tag{4}$$

where

$$\mu = (z^{2\delta_N} - \beta)/(1-\beta) z^{\delta_N}. \tag{5}$$

This gives explicit values for the normalized forces at the two ribs at the extreme right, i.e. $E_{N-1} = \mu$ and $E_N = 1$. We will denote the vector $(\mu, 1)$ by $\boldsymbol{x}$.

(ii) *Transfer matrices*

The next step is to rearrange equations [1]–[N] so that the force at any rib is expressed completely in terms of those at neighbouring ribs. We now consider three consecutive equations [n], [$n+1$], [$n+2$] where $2 \leqslant n \leqslant N-2$. Each of these is an equation in $\boldsymbol{A}_m$ of the form (3) for $m = n$, $n+1$, or $n+2$. We define the vector $\boldsymbol{B}$ as

$$\boldsymbol{B} = \boldsymbol{A}_{n+1} - z^{x_{n+1}-x_n}\boldsymbol{A}_n - \gamma_n(\boldsymbol{A}_{n+2} - z^{x_{n+2}-x_n}\boldsymbol{A}_n),$$

where

$$\gamma_n = \frac{z^{-x_{n+1}} - z^{x_{n+1}-2x_n}}{z^{-x_{n+2}} - z^{x_{n+2}-2x_n}}. \tag{6}$$

It is easily verified that $\boldsymbol{B}$ has only three non-zero entries. Further, since $\boldsymbol{B}$ is a linear combination of the vectors $\boldsymbol{A}_m$, we have $\boldsymbol{B}\cdot\boldsymbol{F} = 0$. Specifically we can write

$$\omega_n F_n + \omega_n' F_{n+1} + \omega_n'' F_{n+2} = 0. \tag{7}$$

For convenience, we have introduced the symbols

$$\left.\begin{aligned} \omega_n &= (1-\beta)\, z^{-x_n}(z^{x_{n+1}} - \gamma_n z^{x_{n+2}}), \\ \omega_n' &= (\beta - z^{2x_{n+1}-2x_n}) - \gamma_n z^{x_{n+2}}(z^{-x_{n+1}} - z^{x_{n+1}-2x_n}), \\ \omega_n'' &= z^{x_{n+2}}(z^{-x_{n+1}} - z^{x_{n+1}-2x_n}) - \gamma_n(\beta - z^{2x_{n+2}-2x_n}). \end{aligned}\right\} \tag{8}$$

From this we can write $F_n = \alpha_n' F_{n+1} + \alpha_n'' F_{n+2}$,

where $\alpha_n' = -\omega_n'/\omega_n$ and $\alpha_n'' = -\omega_n''/\omega_n$. The transfer matrix equation is then given by

$$(F_n, F_{n+1}) = P_n(F_{n+1}, F_{n+2}), \tag{9}$$

where P_n is the matrix

$$P_n = \begin{pmatrix} \alpha_n' & \alpha_n'' \\ 1 & 0 \end{pmatrix}. \tag{10}$$

These coefficients may be required in terms of rib locations x_n, displacements u_n, or spacings δ_n. Here we need only the dependence upon δ_n:

$$\alpha_n' = -\frac{\beta z^{-(\delta_{n+1}+\delta_{n+2})} + (2-\beta)\, z^{\delta_{n+1}+\delta_{n+2}} - z^{\delta_{n+1}-\delta_{n+2}} - z^{\delta_{n+2}-\delta_{n+1}}}{(1-\beta)\,(z^{-\delta_{n+2}} - z^{\delta_{n+2}})} \tag{11a}$$

and

$$\alpha_n'' = -\frac{z^{\delta_{n+1}} - z^{-\delta_{n+1}}}{z^{\delta_{n+2}} - z^{-\delta_{n+2}}}. \tag{11b}$$

Equations (11) depend on the two random variables δ_{n+1}, δ_{n+2}; the corresponding expressions in terms of rib displacements are more complicated in that they depend upon the three random variables u_n, u_{n+1}, u_{n+2}. Note that the quantity $z^{-\delta_{n+2}} - z^{\delta_{n+2}}$ in the denominator of both terms vanishes when the bay length times frequency is a multiple of π. We denote by δ_{crit} the value of δ where this occurs. Despite these singularities, there is no dramatic change of amplitude at such points, as will be shown in §4. For the moment we will assume that $z^{-\delta_{n+2}} \neq z^{\delta_{n+2}}$.

From the above equations we obtain the normalized forces, which are more conveniently written in pairs:

$$(E_m, E_{m+1}) = P_m \ldots P_{N-2}(\boldsymbol{x}) \tag{12}$$

for $N-2 \leqslant m \leqslant 2$, where $\boldsymbol{x}$ again denotes the vector $(\mu, 1)$.

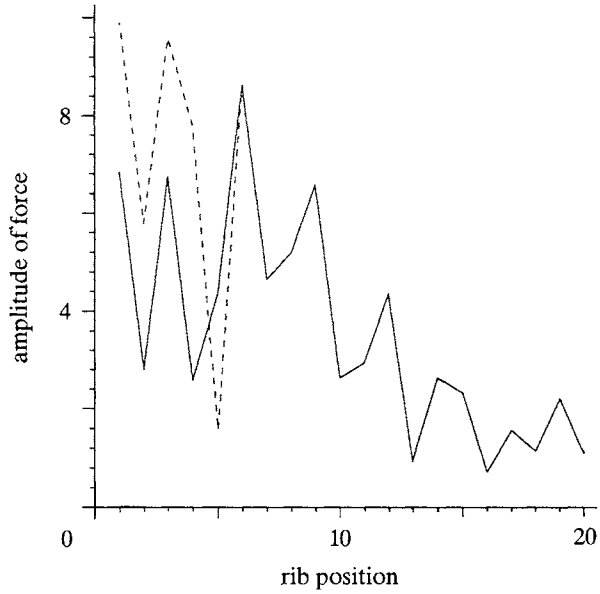

Figure 1. Amplitude of the force $|E_n|$ as a function of n along two arrays of length 20 which differ only in the position of the 5th rib.

(iii) *Forces at each end rib and completion of the solution*

It remains only to find the forces at the first (the driven rib) and last ribs. The normalized driving force E_1 can be found from any of the equations [2] to [N]. From [2] for example we obtain

$$E_1 = -z^{-\delta_2}\left[\beta E_2 + \sum_{i=3}^{N} z^{x_i - x_2} E_i\right]. \tag{13}$$

Finally the normalizing factor, i.e. the end force F_N, is obtained by dividing equation [1] through by F_N, and taking the reciprocal of each side:

$$F_N = \left[\beta E_1 + \sum_{i=2}^{N} z^{x_i - x_1} E_i\right]^{-1}, \tag{14}$$

where the values E_n are given by (12) and (13). Since $F_m = E_m F_N$ for all m, this completes the solution.

Equations (12)–(14) represent an exact solution to the problem (2) for an arbitrary configuration of ribs. The action of the matrix with random elements of order 1 everywhere thus reduces to nearest-neighbour coupling apart from the constant multiple F_N throughout and the driving force F_1. Note that direct inversion of the matrix A is inherently sensitive to numerical error in such systems, and is computationally prohibitive for large arrays (see Sobnack 1991). Both of these difficulties are overcome by the above solution.

(iv) *Some examples*

It is now clear that if a rib in any system is relocated, only the forces to the left are affected, apart from a change in the multiplying factor F_N. An illustration of this is given in figure 1, which shows the normalized forces E_n along two irregular arrays of 20 ribs, identical except for a shift in position of the 5th rib. (The forces are shown here as functions of rib-position.)

We conclude this part with two more examples exhibiting the difference between the behaviour in stop and pass band frequencies. Figure 2 shows the response at the mid-pass band frequency $\frac{5}{6}\pi$, along an array of 30000 ribs with very slight disorder $\Delta = 0.05$. This shows both long-range localization, and many local fluctuations of several orders of magnitude. The full array (showing the force at every 50th rib), is given in (*a*), and in (*b*) is a 'short' section of 500 ribs. By contrast, figure 3 shows the response for much larger disorder, $\Delta = 0.8$, at the stop band frequency $\frac{1}{2}\pi$. In these figures, the horizontal axis represents rib position. Further illustrations are given in §4, where the response is considered in more detail.

(*b*) *Average transfer matrix*

We now calculate the average $P = \langle P_n \rangle$, and briefly examine its eigenvectors and eigenvalues. This will later enable us to characterize the localization length in those regimes in which the effects of disorder are not too significant.

We consider model 2, and assume here that $\Delta < \pi/\phi - 1$, so that singularities in (11*a*), (11*b*) are excluded. To specify $\langle P_n \rangle$, we need the mean matrix coefficients. Define $\alpha' = \langle \alpha'_n \rangle$, $\alpha'' = \langle \alpha''_n \rangle$. Since these coefficients are functions of two independent random variables δ_{n+1}, δ_{n+2}, each is given by a double integral. (For statistical model 1, the coefficients are functions of three successive random variables. The resulting triple integrals appear to be intractable, although they may be reduced to a single integral which is easily treated approximately for small disorder.) Let $\epsilon_n = \delta_n - 1$, so that the random variables ϵ_n are uniform in $[-\Delta, \Delta]$. Since little confusion can arise here, we will drop the subscript n. The probability integrals are evaluated in the appendix. From equation (11*a*), it is not difficult to see that α' can be written

$$\alpha' = -\frac{1}{1-\beta}\left[(\beta\langle z^{-\delta}\rangle - \langle z^{\delta}\rangle)\left\langle \frac{z^{-\delta}}{z^{-\delta}-z^{\delta}}\right\rangle + ([2-\beta]\langle z^{\delta}\rangle - \langle z^{-\delta}\rangle)\left\langle \frac{z^{\delta}}{z^{-\delta}-z^{\delta}}\right\rangle\right].$$

From (A 2)–(A 5),

$$\alpha' = -\frac{\sin(\phi\Delta)}{(1-\beta)\,\phi\Delta}\left[(\beta z^{-1}-z)\left(1-\frac{\ln(1-z^{2+2\Delta})-\ln(1-z^{2-2\Delta})}{4\mathrm{i}\phi\Delta}\right)\right.$$
$$\left. -([2-\beta]z-z^{-1})\left(1-\frac{\ln(z^{-2+2\Delta}-1)-\ln(z^{-2-2\Delta}-1)}{4\mathrm{i}\phi\Delta}\right)\right]. \quad (15)$$

The second coefficient is slightly easier to obtain:

$$\alpha'' = (\langle z^{\delta}\rangle - \langle z^{-\delta}\rangle)\langle z^{-\delta}/(z^{-2\delta}-1)\rangle,$$

which, using (A 2), (A 3) and (A 6), gives

$$\alpha'' = \frac{\sin(\phi\Delta)}{4\mathrm{i}\phi^2\Delta^2}(z-z^{-1})\left[\ln\left(\frac{-z+z^{\Delta}}{-z-z^{\Delta}}\right)-\ln\left(\frac{-z+z^{-\Delta}}{-z-z^{-\Delta}}\right)\right]. \quad (16)$$

The eigenvalues are given by the roots of the equation

$$\lambda^2 - \alpha'\lambda - \alpha'' = 0.$$

Thus
$$\lambda_i = \tfrac{1}{2}(\alpha' \pm \sqrt{(\alpha'^2 + 4\alpha'')}) \quad (17)$$

where $i = 1, 2$ and $i = 1$ corresponds to the plus sign before the square root. The corresponding eigenspaces are then represented by the vectors

$$\boldsymbol{y}_i = (\lambda_i, 1). \quad (18)$$

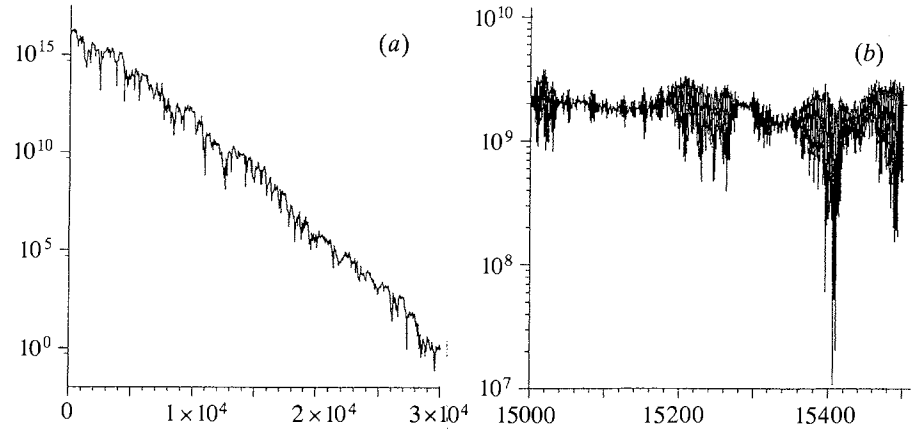

Figure 2. (*a*) Log-linear graph of the force along an array of 30000 ribs, at the mid-pass band frequency $\phi = \frac{5}{6}\pi$, and $\Delta = 0.05$, showing every 50th value; (*b*) the forces on a short section of 500 ribs in the middle of the same array.

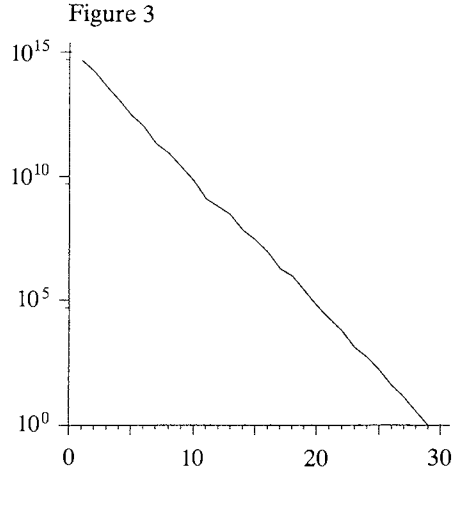

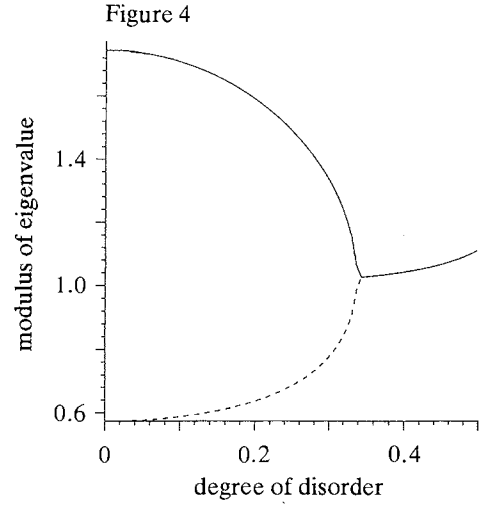

Figure 3. Force along an array of length 30, at the mid-stop band frequency $\frac{2}{3}\pi$, for large disorder $\Delta = 0.8$.

Figure 4. Moduli of the two eigenvalues of the averaged transfer matrix $\langle P_n \rangle$, as functions of disorder Δ, at the stop band frequency 2.0.

Since the eigenvalues in the periodic case completely determine the band structure, it is interesting to consider the effect upon them of disorder. In the pass band the moduli of the eigenvalues of $\langle P \rangle$ remain equal but increase from one. At stop band frequencies, the moduli of the eigenvalues eventually approach each other as the disorder increases. The larger eigenvalue decreases, and it will be seen that this corresponds to slower exponential decay as the disorder increases. These moduli are seen in figure 4 as functions of Δ at $\phi = 2.0$. As the frequency approaches the band edge the eigenvalues coalesce at a decreasing value of disorder.

4. Disorder and localization

We now consider the main effects of disorder on the typical response of the structure, and in particular we aim to explain the distinct character of response found at different frequencies. We shall show also that in one region, in which the decay is smooth, the decay rate can be characterized by the eigenvalues of the mean transfer matrix. The singularities which arise in the transfer matrix coefficients will be discussed in §4*b* below.

(*a*) *Régimes of localization*

Localization is usually defined as an asymptotic property as $n \to \infty$:

$$n^{-1} \ln |F_n| \sim \gamma. \tag{19}$$

Here, γ is some fixed function of frequency and disorder (see for example figure 2), which we refer to as the decay rate. (We can also consider the *decay length* $1/\gamma$). Sobnack (1991) studied the *ensemble averaged* quantity

$$n^{-1} \langle \ln |F_n| \rangle = \gamma'. \tag{20}$$

Equation (20) is useful for arrays of fixed length N and in practice yields the same decay rate as (19) for sufficiently large N. Note that (20) is not strictly independent of n, and for sufficiently small N or Δ the variations along the array can overshadow the decay. Nevertheless, in simulations (20) converges remarkably smoothly to a constant value even for small N. Neither quantity, however, describes detailed features of the response.

The existence of two markedly different régimes of localization has been seen in figures 2 and 3. There are regions of smooth and of fluctuating decay, which correspond roughly to the stop and pass bands respectively. In addition Sobnack (1991) found from numerical simulations that the average stop band decay rate (20) is affected little by structural disorder. These properties have essentially the same origins, which lie in the properties of the eigenvalues of the transfer matrices. The behaviour along the array can therefore be understood by examining the properties of each transfer matrix.

Consider for the moment the transfer matrix P_n (equation (10)) as a 'canonical' function of the random variable δ_{n+1}. We denote the eigenvalues of P_n by $\lambda_i^{(n)}$, so that

$$\lambda_i^{(n)} = \tfrac{1}{2}(\alpha_n' \pm \sqrt{(\alpha_n'^2 + 4\alpha_n'')}) \tag{21}$$

for $i = 1, 2$, where $i = 1$ corresponds to the plus sign. The corresponding eigenvectors are

$$\boldsymbol{y}_i^{(n)} = (\lambda_i^{(n)}, 1). \tag{22}$$

Throughout the pass bands the eigenvalues $\lambda_1^{(n)}$, $\lambda_2^{(n)}$ have equal modulus even for large disorder, while in most of the stop band one of the values remains dominant as disorder increases. These properties and their effects closely echo the periodic case (see §2). Figure 5 shows the ratio of the eigenvalues of P_n as a function of rib spacing and frequency. Here the rib spacing, represented by δ_{n+1}, increases from 1 (no disorder) to 1.3, and δ_{n+2} is fixed at 1. The results are qualitatively independent of the specific value of δ_{n+2}. Remarkably little change takes place with change in spacing. The sharp increase which marks the band edge in the regular case remains, moving gradually into the stop band as the disorder increases. We note, however, that the product of the eigenvalues is no longer unity.

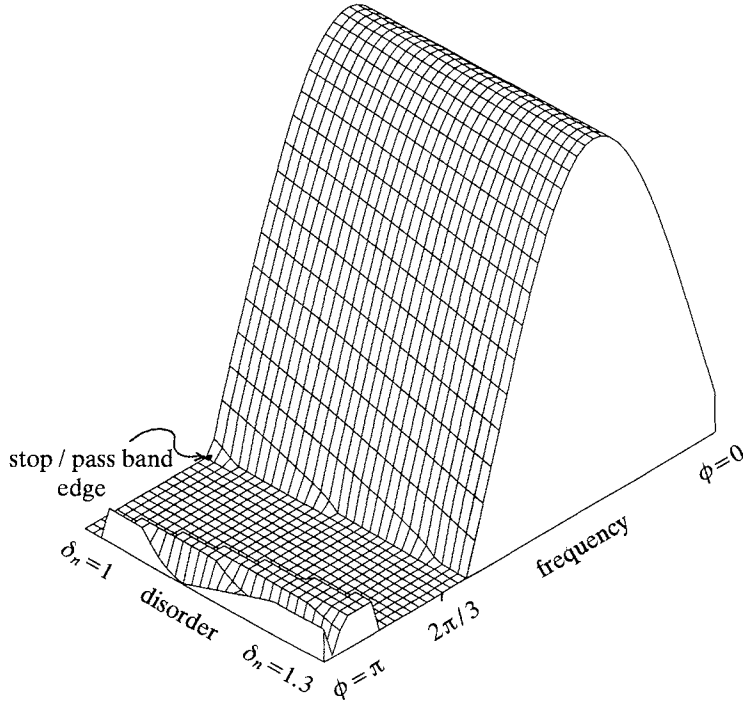

Figure 5. Ratio of the eigenvalues of P_n as a function of rib spacing and frequency. Frequency increases from 0 to π from right to left. The disorder, represented by rib-spacing δ_n, increases from 0 (i.e. $\delta_n = 1$) to 0.3 ($\delta_n = 1.3$), with δ_{n+1} fixed at 1. The base level of the graph is at unity. Values in the triangular region $\delta_n \geqslant \delta_{\text{crit}}$ beyond the singularity have been arbitrarily cut off at 2.0.

The second effect is not as sharply defined but is also important: along the array the distribution of eigenvalues, and therefore (from (22)) that of the eigenvectors, is relatively narrow throughout the stop band. This occurs because the dominant eigenvalues change very little at stop band frequencies as the disorder increases, and is clear from figure 6, which shows the ratio $|\lambda_i^{(n)}/\lambda_i|$ as a function of frequency and disorder. Here λ_i is the corresponding eigenvalue for the regular array, so this quantity measures the extent to which the dominant eigenvalues change with disorder. The effect of this is illustrated in figure 7, which compares variation of the dominant eigenvalue along a typical array at stop and pass band frequencies. The lower curve, corresponding to the mid-pass band frequency, shows variation which is greater than that of the mid-stop band, shown in the upper curve, by roughly an order of magnitude. The eigenvalues of the mean transfer matrix $\langle P \rangle$ are also shown, indicated by the straight lines.

To understand the consequence of this, consider the trajectory of any two-dimensional vector (i.e. forces at two adjacent ribs) under the action of successive matrices P_n. In the stop band, where $\lambda_i^{(n)}$, say, is the dominant value, P_n acts almost like the projection onto $\boldsymbol{y}_i^{(n)}$, multiplied by $\lambda_i^{(n)}$. The vectors $\boldsymbol{y}_i^{(n)}$ lie in a similar direction for all n, so subsequent matrices simply attract the trajectory into a narrow cone of directions where it becomes trapped, increasing in modulus with the $\lambda_i^{(n)}$s. In the pass band, however, there is no such preferred region, and just as in the periodic case this results in fluctuations along the array, which are increased here by random variations in the eigenvectors. The situation is shown schematically in figure 8*a* (stop

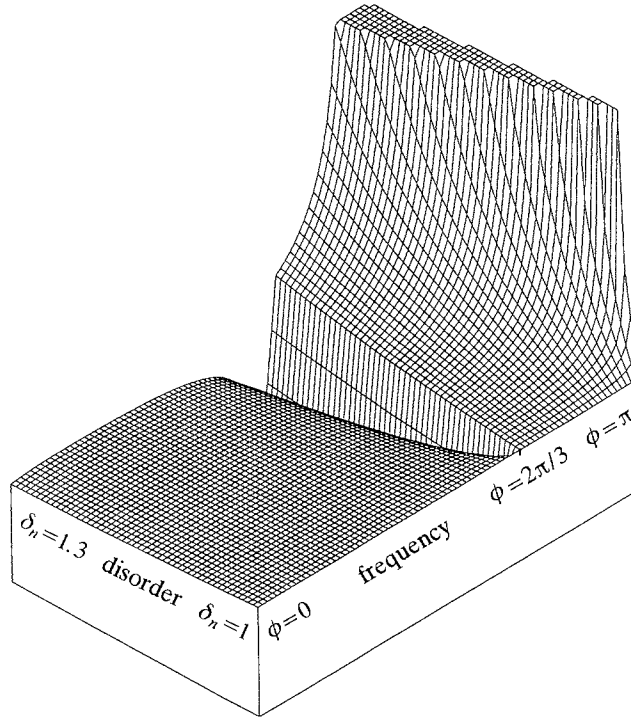

Figure 6. Ratio $|\lambda_i^{(n)}/\lambda_i|$ as a function of frequency and disorder, where λ_i and $\lambda_i^{(n)}$ are the dominant eigenvalues for disorder equal to zero and δ_n respectively. δ_n again increases from 1 to 1.3, and the frequency goes from zero to π. Where the values are level they are approximately one. The values in the region $\delta_n \geqslant \delta_{\text{crit}}$ have again been limited to 2.0.

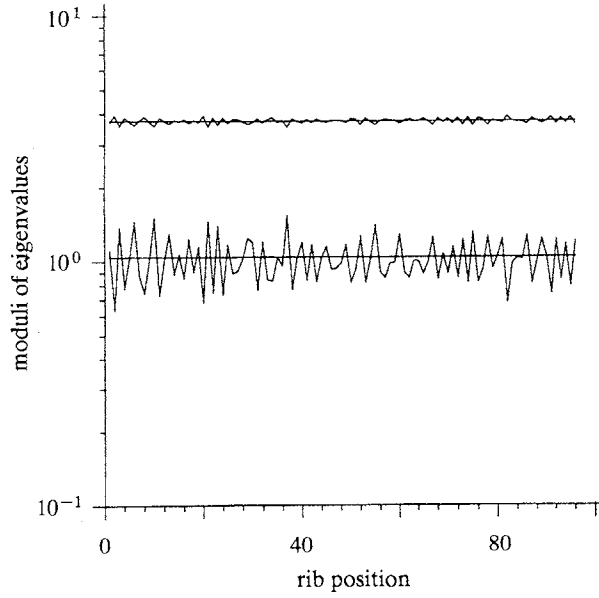

Figure 7. Moduli of the dominant eigenvalue of transfer matrices P_n as functions of rib-position n along a typical array of length 100, at two frequencies. The upper curve (slight variation) is at the mid-stop band, and the lower curve (large variation) is the mid-pass band. The straight lines represent the eigenvalues of the averaged matrices $\langle P_n \rangle$.

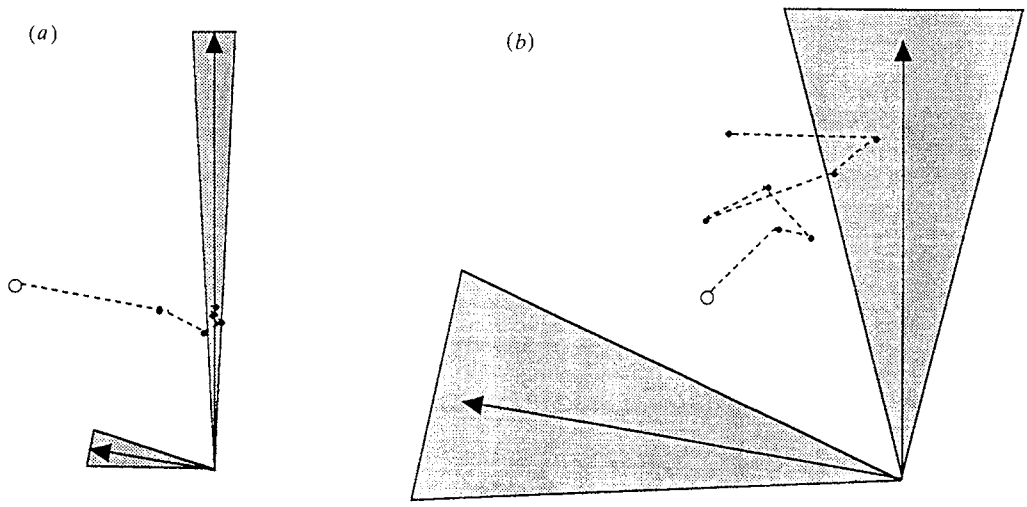

Figure 8. Schematic view of the action of the transfer matrices (*a*) in the stop band and (*b*) in the pass band. The arrows represent typical eigenvectors with lengths corresponding to the magnitude of the respective eigenvalues, normalized so that the vertical eigenvector has unit eigenvalue. The shaded areas indicate the spread of angles of the eigenvectors as they change randomly along the array. The trajectory of one initial vector under the action of the first few matrices is shown in each case.

band) and 8*b* (pass band). Here the arrows represent typical eigenvectors (which will not in general be orthogonal), with lengths corresponding to the magnitude of the respective eigenvalues. The shaded areas indicate the spread of angles that occur as the transfer matrices, and therefore the eigenvectors, change randomly along the array. For clarity, the actions of the matrices shown here have been normalized so that the vertical eigenvector has length unity. A typical trajectory of an arbitrarily chosen vector under the action of the first few matrices is shown in each case.

Some further features emerge from this. First, it suggests that where the response decays smoothly, the decay rate can be characterized by the eigenvalues of the mean matrix $\langle P_n \rangle$. This is confirmed by the comparison, in figure 9, between the decay length as a function of frequency and the quantity $1/\ln|\lambda_i|$, where λ_i is the modulus of the dominant eigenvalue. Here $\Delta = 0.5$, and the zero-disorder case is included for comparison. Secondly, since the dominant eigenvalue decreases in the stop band, the effect of disorder there is to increase the localization length. This is also clear from figure 9. We note that since disorder tends to decrease localization in the stop bands, the decay rate against frequency curve for the random case crosses that for the regular case at some point in the stop band, for every non-zero Δ. At such frequencies, the decay length at first increases with Δ and then decreases again, crossing the value it has in the regular array.

Finally, we recall that for a regular array the pass band response varies rapidly with frequency. Although irregularity eliminates these pass bands, the response of any given array retains a high sensitivity to frequency. Figure 10 shows the response at two frequencies, $\phi = 3.1$ and $\phi = 3.2$, in a small neighbourhood of the band-edge at π. The array consists of 50 ribs with small disorder, $\Delta = 0.05$. Although the change in decay rate is particularly sharp because the interval includes the band edge, similar changes in the details of the pattern are found throughout the frequency range. A further illustration of frequency dependence is given in figure 11. This shows

Figure 9

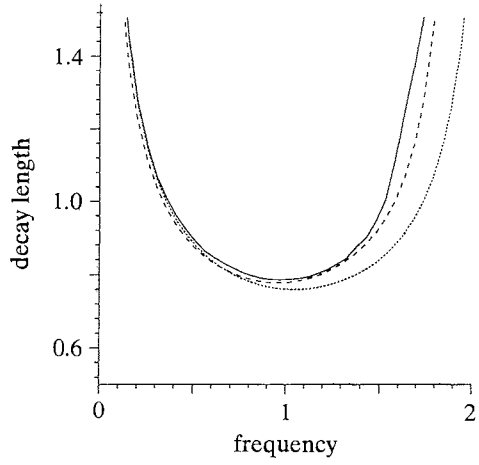

Figure 10

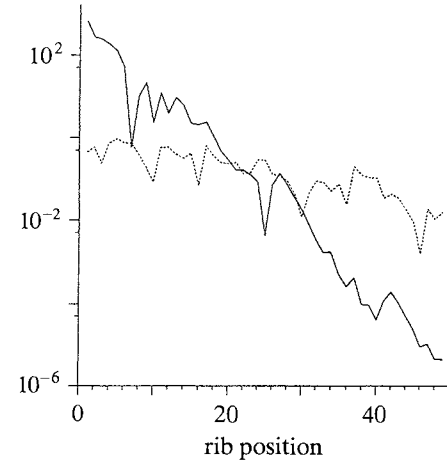

Figure 9. Comparison between the decay length (full line) as a function of frequency and the quantity $1/\ln|\lambda_i|$ (dashed line), where λ_i is the dominant eigenvalue of $\langle P \rangle$. The decay length was found by averaging over many numerical simulations. The decay length for a regular array is also shown (dotted line).

Figure 10. The modulus of the response at two frequencies along the same array of 50 ribs: (*a*) $\phi = 3.1$ (dotted line), and (*b*) $\phi = 3.2$ (full line).

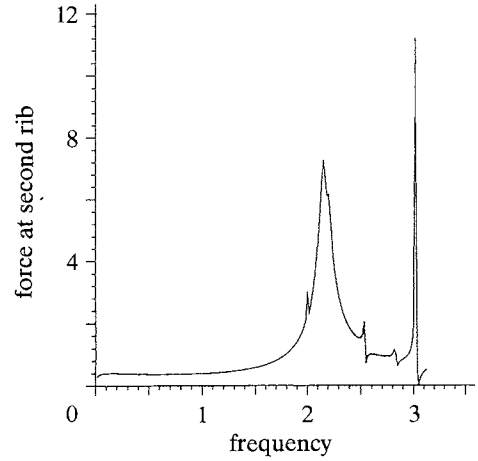

Figure 11. The modulus of the force at the second rib in a fixed array of length 10 with disorder $\Delta = 0.2$, as the frequency changes from 0 to π.

the amplitude of the force at a single rib (the second) as a function of ϕ, from 0 to π, for larger disorder $\Delta = 0.2$ in a fixed array of length 10. The smooth behaviour in the stop band and the extremely rapid amplitude changes in the pass band are typical of the results obtained.

(*b*) *Transfer matrix singularities*

In §3, we noted that there are conditions under which the elements α'_n and α''_n of the transfer matrix P_n can become singular. This occurs when (see equation (11))

$$z^{-\delta_{n+2}} - z^{\delta_{n+2}} \equiv -2\mathrm{i}\sin\phi\delta_{n+2} = 0.$$

Physically, this condition arises when the distance between ribs $n+1$ and $n+2$ is an integer multiple of the wavelength, and so corresponds to a resonance condition in a system without fluid loading. As we now show, however, the fluid loaded system exhibits no resonance phenomenon at these frequencies.

To determine the behaviour of the solution as $\sin\phi\delta_{n+2}\to 0$, we must consider the explicit dependence of the solution on the variable δ_{n+2}. Since only P_n and P_{n+1} depend on δ_{n+2}, it suffices to consider the matrix product

$$\boldsymbol{M} = P_n P_{n+1} = \begin{bmatrix} M_{11} & M_{12} \\ M_{21} & M_{22} \end{bmatrix}.$$

The matrix $\boldsymbol{M}$ takes the vector (F_{n+2}, F_{n+3}) to the vector (F_n, F_{n+1}). Using equations (10) and (11), we find that the elements M_{ij} are given by

$$\left.\begin{aligned}
M_{11} &= \frac{(z^{-\delta_{n+1}} - z^{\delta_{n+1}})(z^{-\delta_{n+2}} - z^{\delta_{n+2}})}{(1-\beta)^2} - \frac{z^{-\delta_{n+1}}z^{-\delta_{n+2}} - z^{\delta_{n+2}}z^{\delta_{n+1}}}{1-\beta} \\
&\quad - \frac{(z^{-\delta_{n+1}} - z^{\delta_{n+1}})(z^{-\delta_{n+3}}z^{-\delta_{n+2}} - z^{\delta_{n+2}}z^{\delta_{n+3}})}{(1-\beta)(z^{-\delta_{n+3}} - z^{\delta_{n+3}})} \\
&\quad + \frac{z^{-\delta_{n+2}}z^{-\delta_{n+1}}z^{-\delta_{n+3}} - z^{\delta_{n+2}}z^{\delta_{n+1}}z^{\delta_{n+3}}}{(z^{-\delta_{n+3}} - z^{\delta_{n+3}})}, \\
M_{12} &= \frac{(z^{-\delta_{n+1}} - z^{\delta_{n+1}})(z^{-\delta_{n+2}} - z^{\delta_{n+2}})}{(1-\beta)(z^{-\delta_{n+3}} - z^{\delta_{n+3}})} - \frac{z^{-\delta_{n+1}}z^{-\delta_{n+2}} - z^{\delta_{n+2}}z^{\delta_{n+1}}}{(z^{-\delta_{n+3}} - z^{\delta_{n+3}})}, \\
M_{21} &= \frac{z^{-\delta_{n+3}}z^{-\delta_{n+2}} - z^{\delta_{n+2}}z^{\delta_{n+3}}}{(z^{-\delta_{n+3}} - z^{\delta_{n+3}})} - \frac{(z^{-\delta_{n+2}} - z^{\delta_{n+2}})}{(1-\beta)}, \\
M_{22} &= -\frac{(z^{-\delta_{n+2}} - z^{\delta_{n+2}})}{(z^{-\delta_{n+3}} - z^{\delta_{n+3}})}.
\end{aligned}\right\} \tag{23}$$

Equations (23) show that the elements of the matrix product $P_n P_{n+1}$ remain bounded for all values of δ_{n+2}. Since the elements of P^n become infinite in the limit as $\sin\phi\delta_{n+2}\to 0$, the matrix $\boldsymbol{M}$ provides a convenient means to evaluate the solution when $\sin\phi\delta_{n+2} \ll 1$.

To understand intuitively why $\boldsymbol{M}$ remains bounded, we can also interpret the action of the matrices P_n and P_{n+1} geometrically. Equations (11) can be used to show that in the limit as $\sin\phi\delta_{n+2}\to 0$,

$$P_{n+1} \to \begin{bmatrix} 1 & 0 \\ 1 & 0 \end{bmatrix}.$$

Thus in this limit, P_{n+1} is a projection onto the vector $(1,1)$, so that when $\sin\phi\delta_{n+2} = 0$, $F_{n+1} = F_{n+2}$. The one-dimensional span of this vector is the only subspace which remains bounded under the action of P_n in the limit. (More precisely, $P_n \boldsymbol{y}$ tends to infinity for all $\boldsymbol{y}$ except multiples of $(1,1)$.)

5. Conclusions

We have obtained an exact solution for the forces along an irregular array of ribs in a fluid-loaded membrane, which is valid in the approximation of purely subsonic-surface wave coupling. The solution is written in the form of a product of transfer

matrices. This formulation allows us to explain the marked sensitivity of the solution to frequency including the two distinct régimes of localization behaviour previously observed in numerical simulation (Sobnack 1991; Photiadis 1992). We have shown that this frequency dependence has the same roots as the stop and pass bands of the regularly ribbed structure.

Two important problems remain. The first is to quantify the localization rate analytically for any degree of disorder. The second is to study localization phenomena under the action of a Green function with longer-range acoustic coupling.

The authors thank Professor D. G. Crighton and Dr M. B. Sobnack for helpful discussions, and the referees for the discovery of a number of errors in the manuscript. This work has been carried out with financial support from the U.K. Natural Environmental Research Council and from the U.S. Office of Naval Research (code N0014-92-J-1035).

Appendix A

In this appendix we calculate some of the quantities required for the average transfer matrix. As in §3, define $\epsilon_n = \delta_n - 1$. Wherever possible the subscript will be dropped. Any function f of the uniformly distributed random variable ϵ has mean

$$\langle f(\epsilon)\rangle = \frac{1}{2\Delta}\int_{-\Delta}^{\Delta} f(X)\,\mathrm{d}X. \tag{A 1}$$

We first evaluate the averages $\langle z^{\delta}\rangle$ and $\langle z^{-\delta}\rangle$. The first of these can be written

$$\begin{aligned}\langle z^{\delta}\rangle &= z\langle z^{\epsilon}\rangle \\ &= z\left[\frac{1}{2\Delta}\int_{-\Delta}^{\Delta} \mathrm{e}^{\mathrm{i}\phi X}\,\mathrm{d}X\right] = \frac{z}{2\mathrm{i}\phi\Delta}(\mathrm{e}^{\mathrm{i}\phi\Delta} - \mathrm{e}^{-\mathrm{i}\phi\Delta}),\end{aligned}$$

so that

$$\langle z^{\delta}\rangle = z\sin(\phi\Delta)/\phi\Delta. \tag{A 2}$$

Similarly

$$\langle z^{-\delta}\rangle = z^{-1}\sin(\phi\Delta)/\phi\Delta. \tag{A 3}$$

We need to calculate three further quantities. The first is the average of the expression

$$z^{-\delta}/(z^{-\delta} - z^{\delta}) = 1/(1 - \mathrm{e}^{2\mathrm{i}\phi + 2\mathrm{i}\phi\epsilon}).$$

Now we can write

$$(1 - \mathrm{e}^{2\mathrm{i}\phi + 2\mathrm{i}\phi X})^{-1} = \frac{\mathrm{d}}{\mathrm{d}X}\left(X - \frac{\ln[1 - \mathrm{e}^{2\mathrm{i}\phi + 2\mathrm{i}\phi X}]}{2\mathrm{i}\phi}\right),$$

and thus, by (A 1),

$$\begin{aligned}\left\langle \frac{z^{-\delta}}{z^{-\delta} - z^{\delta}}\right\rangle &= \frac{1}{2\Delta}\int_{-\Delta}^{\Delta} \frac{1}{1 - \mathrm{e}^{2\mathrm{i}\phi + 2\mathrm{i}\phi X}}\,\mathrm{d}X \\ &= \frac{1}{4\mathrm{i}\phi\Delta}[2\mathrm{i}\phi X - \ln(1 - z^{2X+2})]_{-\Delta}^{\Delta}.\end{aligned} \tag{A 4}$$

Next, since $z^{\delta}/(z^{-\delta} - z^{\delta})$ is the complex conjugate of $-z^{-\delta}/(z^{-\delta} - z^{\delta})$, we obtain

$$\left\langle \frac{z^{\delta}}{z^{-\delta} - z^{\delta}}\right\rangle = -\frac{1}{4\mathrm{i}\phi\Delta}[2\mathrm{i}\phi X + \ln(1 - z^{-2X-2})]_{-\Delta}^{\Delta}. \tag{A 5}$$

Finally, we need to find

$$\left\langle \frac{z^{-\delta}}{z^{-2\delta}-1} \right\rangle = z \left\langle \frac{1}{z^{\epsilon}-z^{2}z^{-\epsilon}} \right\rangle.$$

Similarly to the above, or applying Gradshteyn & Ryzhik (1965, eqn 2.313, p. 92), we eventually obtain

$$\left\langle \frac{z^{-\delta}}{z^{-2\delta}-1} \right\rangle = \frac{1}{4\mathrm{i}\phi\Delta}\left[\ln\left(\frac{-z+z^{X}}{-z-z^{X}}\right)\right]_{-\Delta}^{\Delta}. \tag{A 6}$$

The branch cut of the above complex logarithm is, as usual, taken along the negative real axis, and the imaginary part defined to lie in $[-\pi, \pi]$. All logarithms are thus defined unambiguously since each of the arguments lies in the right half of the complex plane.

References

Crighton, D. G. 1983 The Green function of an infinite, fluid loaded membrane. *J. Sound Vib.* **86**, 411–433.

Crighton, D. G. 1984 Transmission of energy down periodically ribbed elastic structures under fluid loading. *Proc. R. Soc. Lond.* A **394**, 405–436.

Crighton, D. G. 1989 The 1988 Rayleigh Medal Lecture. Fluid loading – the interaction between sound and vibration. *J. Sound Vib.* **133**, 1–27.

Crighton, D. G. & Maidanik, G. 1981 Acoustic and vibration fields generated by ribs on a fluid-loaded panel. I. Plane-wave problems for a single rib. *J. Sound Vib.* **75**, 437–452.

Eatwell, G. P. & Willis, J. R. 1982 The excitation of a fluid-loaded plate stiffened by a semi-infinite array of beams. *IMA J. appl. Math.* **29**, 247–270.

Gradshteyn, I. S. & Ryzhik, I. M. 1965 *Tables of integrals, series and products*, 4th edn. New York: Academic Press.

Mace, B. R. 1980 Periodically stiffened fluid-loaded plates. II. Response to line and point forces. *J. Sound Vib.* **73**, 487–504.

Papoulis, A. 1981 *Probability, random variables and stochastic processes.* New York: McGraw-Hill.

Photiadis, D. G. 1992 Anderson localization of one-dimensional wave propagation on fluid-loaded plate. *J. Acoust. Soc. Am.* **91**, 771–780.

Photiadis, D. G. 1992 The effect of irregularity on the scattering of acoustic waves from a ribbed plate. *J. Acoust. Soc. Am.* **91**, 1897–1903.

Sobnack, M. B. 1991 Fluid loading and Anderson localisation. Ph.D. thesis, University of Cambridge.

Sobnack, M. B. & Crighton, D. G. 1993 Effect of an isolated irregularity on the transmission of energy down a periodically ribbed fluid-loaded elastic structure. *Proc. R. Soc. Lond.* A **441**, 473–494.

Sobnack, M. B. & Crighton, D. G. 1994 Anderson localization effects in the transmission of energy down an irregularly ribbed fluid-loaded structure. *Proc. R. Soc. Lond.* A. **444**, 185–200.

Spivack, M. 1991 Wave propagation in finite periodically ribbed structures with fluid loading. *Proc. R. Soc. Lond.* A **435**, 615–634.

Received 26 October 1992; accepted 23 June 1993